Journal of Rock Mechanics and Geotechnical Engineering 18 (2026) 4081–4093

Contents lists available at ScienceDirect

Journal of Rock Mechanics and Geotechnical Engineering

journal homepage: www.jrmge.cn

Full Length Article

Reinforcement and carbon dioxide sequestration in soft soil treated with triethanolamine-modified ternary eco-binder

Zhuoyu Duan [a], Dongxing Wang [a,b,c,*], Yong Zou [a], Hao Luo [a]

[a] School of Civil Engineering, Wuhan University, 8 Dong Hu South Road, Wuhan, 430072, China
[b] Key Laboratory of Rock Mechanics in Hydraulic Structural Engineering of the Ministry of Education, Wuhan University, Wuhan, 430072, China
[c] School of Civil Engineering, University of South China, Hengyang, 421001, China

ARTICLE INFO

Article history:
Received 16 February 2025
Received in revised form
15 June 2025
Accepted 18 August 2025
Available online 5 November 2025

Keywords:
Soft soil
Carbonation
Industrial wastes
Solidification
Triethanolamine

ABSTRACT

To realize the soil reinforced through the carbonation of ternary binder under ambient pressure and mild conditions, the present study introduces triethanolamine (TEA), which serves as an effective carbonation accelerator. Through the unconfined compressive strength (UCS) test, the soft soil solidified with ternary eco-binder consisting of ground granulated blast-furnace slag (GGBS), metakaolin (MK), and calcium carbide residue (CCR), subjected to carbonation, is investigated. The effect of TEA on the carbonation of soil is evaluated by the UCS and the CO_2 mineralization. This study clarifies the influence factors, including the initial water content, TEA dosage, binder constituent ratio, and content. The optimal binder constituent ratio for the strength growth and carbonation efficiency of carbonated soil is approximately 4:4:2 for GGBS, CCR, and MK, respectively. The incorporation of TEA at a low dosage (<0.15 %) enhances the strength of carbonated soil, whereas the high dosages impair the strength. The synergistic effect of TEA and carbonation further improves the strength and compressibility of soil. The soil with 1.5 % TEA carbonated for 7d exhibits a 44.8 % increase in strength compared to that without TEA, which is attributed to a 2.2-fold increase in carbonation efficiency. The addition of TEA accelerates the ion dissolution and CO_2 dispersion, promoting the carbonation reaction in soft soil. Calcite and aragonite precipitate during carbonation, contributing to the strength development of soil. The carbonates phase difference and the pore structure density with different TEA dosages are also demonstrated to be the strength influence factors.

1. Introduction

Grouting and deep mixing, owing to the economic and technical efficiency, are widely adopted in the reinforcement of soft ground, accompanied by a large amount of cement consumption. However, the total CO_2 emission per ton of cement produced is 0.545 t (Shen et al., 2015), which greatly contributes to the global warming. The substitution of eco-binders for Portland cement, commonly used in structure construction and soil solidification, reduces the CO_2 footprint and environmental pollution. Alkaline industrial by-products (IBPs) and other minerals rich in aluminosilicate constitute the primary source of eco-cementitious materials, such as ground granulated blast-furnace slag (GGBS), calcium carbide residue (CCR), phosphogypsum (PG) and metakaolin (MK). These materials form a 3-dimensional (3D) continuous network structure, through the pozzolanic and hydration reactions under alkaline environment (Provis and Bernal, 2014; Liu et al., 2021a; Lang et al., 2025). The application of IBPs and geopolymers in the soil solidification improves variety of soil properties, such as strength, durability, compressibility and the leachability of pollutants (Phetchuay et al., 2016; Li et al., 2023a; Liu et al., 2023; Wang and Wang, 2023).

Carbon capture, utilization and storage (CCUS) is now a promising way to achieve carbon neutrality. Carbonation curing of cement-based materials enhances the properties and sequesters CO_2 (Chen et al., 2019; Zajac et al., 2022). Accelerated carbonation has been applied as a technology to the carbon reduction benefited from the soil solidification using cement and reactive MgO. Yi et al. (2016) incorporated carbonation into reactive MgO-stabilized soil

* Corresponding author. School of Civil Engineering, Wuhan University, 8 Dong Hu South Road, Wuhan, 430072, China
E-mail address: dongxing-wang@whu.edu.cn (D. Wang).

Peer review under responsibility of Institute of Rock and Soil Mechanics, Chinese Academy of Sciences.

https://doi.org/10.1016/j.jrmge.2025.08.023

and demonstrated that the expansive carbonation products of reactive MgO densify the soil particle structure increasing the dry density and strength. According to the life cycle assessments, there are controversies over the climate benefit from cement carbonation, and the reactive MgO emits a higher amount of CO_2 due to the decomposition of magnesite (Ruan and Unluer, 2016; Xi et al., 2016; Van Roijen et al., 2024). In contrast, the widespread use of IBPs in CO_2 mineralization produces calcite and zeolite, realizing the resource utilization of IBPs (Ma et al., 2021; Shin and Kim, 2022). The strength and durability enhancement of sludge solidified with reactive MgO and fly ash can be significantly enhanced through carbonation (Wang et al., 2019a, 2019b). Yu et al. (2021, 2024) utilized steel slag as a binder and subjected solidified soil to a 200 kPa CO_2 atmosphere for 72 h, finding that the total porosity decreased and resistance to dry-wet cycles distinctly enhanced. However, the carbonation efficiency (CE) is limited by the low gas permeability of fine particles, necessitating high air pressure that may induce cracks in the soil. Additionally, the alkaline solid waste used solely has a low carbonation reactivity. To address the aforementioned shortages, Li et al. (2023b) used sodium bicarbonate ($NaHCO_3$) to act as a CO_2 carrier and release CO_3^{2-}, which is much easier than injecting high-pressure CO_2 gas into soil.

Recent studies of the CO_2 mineralization focus on the solid waste dissolution and CO_2 absorption, leading to the proposal of integrated absorption-mineralization (IAM), which relies primarily on the amine solutions (Ji et al., 2018). In the IAM process, the phase transition of CO_2 is contributed by the amine solution, among which the commonly used amine can be classified into primary, secondary, and tertiary amines. The former two species of amines react with CO_2 and form carbamate (R_2NCOO^-) ions, while the tertiary amines, such as triethanolamine (TEA), catalyze the formation of hydroxyl (OH^-) ions in the water relying the lone pair electrons on nitrogen-atoms (Meng et al., 2022). Through the chelation, amines of appropriate concentrate also enhance the dissolution of alkaline minerals constituents of IBPs, and thus help metal cations leaching, which is commonly used in CO_2 mineral sequestration and cement additives (Lu et al., 2020; Wang et al., 2023). Ben et al. (2024) investigated the effect of TEA on external attack on the cement paste, revealing that an increase of TEA accelerates decalcification of C-S-H and promotes the formation of calcite. TEA accelerates or retards the cement strength development depending on its dosage, which is attributed to the combined effects of the promotion of tricalcium aluminate (C_3A) hydration, ettringite formation and the adsorption on the portlandite (Xu et al., 2017; Yaphary et al., 2017).

In terms of the carbonation curing of cement-based materials, the amines represented by TEA were used as CO_2 absorbents to facilitate the cement carbonation. It was confirmed that CO_2-absorbed monoethanolamine (MEA) solutions enhance the strength of cement pastes and bottom ash mortars, which is related to the reduction in macropores (Han et al., 2023). Teune and Schollbach, 2024 used TEA to separate Ca^{2+} from recycled concrete fines and the TEA of 0.2 wt%-1 wt% increases the carbonation degree by 16 %–21 %. The improvement in compressive strength of the cement mortar using CO_2-absorbed TEA solution is attributed to the acceleration and synergistic effect of cement hydration and carbonation (Xin et al., 2024).

To improve the CE under ambient pressure and relatively mild operating conditions, the present study introduces TEA of varying dosages into the soft soil reinforced with ternary eco-binder (i.e. GGBS, CCR and MK) as a carbonation accelerator. The optimal binder constituent ratio, initial water content and the TEA dosage are analyzed concerning the unconfined compressive strength (UCS) and CO_2 mineralization of solidified soil. Besides, the mechanisms underlying the carbonation acceleration and strength improvement impacted by TEA in the soft soil reinforced by ternary eco-binder are explored by scanning electron microscopy (SEM), X-ray diffraction (XRD), thermogravimetric analysis (TGA), pH and zeta potential measurement.

2. Material and methods

2.1. Materials

The soft soil used in this study was obtained from Zhuhai, a coastal city in south China. Table 1 summarizes the basic properties of the soft soil, determined according to ASTM D4318-17e1 (2018), and the initial water content is around 60 %. Fig. 1 shows the grain size distribution of the soft soil, which is tested following ASTM D7928-21e1 (2021), with 3 % sand, 76 % silt and 21 % clay. Given its fine particle distribution and the poor mechanical properties, the soft soil services as an ideal subject for investigation. Before the preparation of specimen, the wet soft soil was dried in ambient conditions, then granulated and passed through a 2-mm sieve.

TEA (99 % purity) was procured from Meryer (Shanghai) Chemical Technology Co., Ltd. GGBS, CCR and MK powders were commercially sourced. The chemical compositions detected by X-ray fluorescence as well as particle size distribution profiles are presented in Table 2 and Fig. 1, respectively. In addition, the MK used here has been sieved through a 1250-mesh sieve, and thus has a rather fine particle size.

2.2. Specimen preparation

The air-dried soft soil was dried at 105 °C for 24 h. Before the specimen preparation, the dry soft soil was mixed with 10 % of its weight in ISO standard sand. Dry soil was mixed with binder powder of various content and ratio of GGBS, CCR and MK (binder constituent ratio) homogeneously. Then, TEA solution was added into the mixture until achieves the designated water content and TEA dosage (the mass percentage of TEA to binder), and stirred for 10 min. Note that the default initial water content for all specimen is 30 %. TEA dosage ranges from 200 ppm to 10000 ppm when TEA was used as accelerator (Heren and Ölmez, 1996). In this study, considering the diluting effect of soil on binders, the magnitudes of TEA dosage were selected as 0, 0.15 %, 0.5 % 1.5 % and 5 %. The well-mixed mixtures, containing designated amount of water, TEA and eco-binder were spread in an enamel tray with a thickness of 30 mm. The mixtures to be carbonated were placed in the carbonation box at (20 ± 2) °C, a relatively humidity (*RH*) of 95 % and a CO_2 concentration of 20 %. After carbonation, the mixture was poured into a steel mold with an inner diameter of 40 mm and a height of 80 mm and statically compacted to the density predetermined by compaction test through a hydraulic jack. For the

Table 1
Basic properties of the soft soil.

Physical property	Value
Specific gravity	2.7
Natural moisture content (%)	45.2
Liquid limit (%)	56.5
Plastic limit (%)	22.1
Plastic index	34.4
Optimal water content (%)	27.4
Maximum dry density (g/cm^3)	1.48
Cohesion (kPa)	15.4
Internal friction angle (°)	5

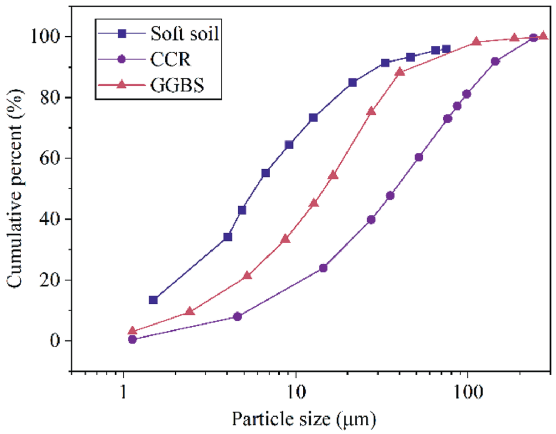

Fig. 1. Particle size distribution of materials used in this study.

Table 2
XRF analysis of materials in this study.

Material	CaO (%)	SiO_2 (%)	Al_2O_3 (%)	MgO (%)	SO_3 (%)	Else (%)	Loss of ignition (%)
GGBS	39.3	33.0	15.0	9.9	1.9	0.1	0.8
CCR	93.2	3.5	1.7	0.2	0.7	0.5	0.2
MK	0.3	53.0	41.5	0.2	0.1	4.9	–

control group, the mixture was compacted and sealed once it was prepared, and then immediately placed in the curing box ((20 ± 2) °C, 95 %*RH*) for the same duration as the carbonation group. Specimens with varying binder compositions are named "*a*P*b*T*c*G*d*C*e*K", which indicates a binder content of *a* %, a TEA dosage of *b* % and a ratio of GGBS: CCR: MK of *c*: *d*: *e*. In addition, specimen names end with the curing time (day). For carbonated specimens, an additional "-M″ followed by the carbonation age (day) is appended to the end of the name to be distinguished from uncarbonated specimens.

2.3. Testing programs

The strength reinforcement was quantified by UCS test with a compression rate of 1 mm/min, and then the fragments were collected for the following tests. The fragments were immediately freeze-dried for the SEM, TGA and XRD tests. SEM tests were carried out using a Zeiss SIGMA field emission SEM device to examine the development of soil microstructure and the morphology of carbonates. To clarify the mineral composition of the specimens, the XRD was conducted through Rigaku Smart-Lab SE X-ray diffractometer with a Cu Kα radiation source. Granulated and freeze-dried specimens were scanned with a step length of 0.02° from 5° to 75°. To investigate the hydration and carbonation products, the TGA was performed using HITACH-STA7300 with a heating rate of 10 °C/min in a nitrogen atmosphere, and the temperature was controlled from 20 °C to 1000 °C.

The oedometer test was conducted using the oedometer following GB/T 4935.1 (2008). The modified soils were compacted in oedometer rings (61.8 mm inner diameter and 20 mm in height). Prior to saturation in a vacuum chamber, the specimens underwent carbonation (or curing) under the conditions mentioned before. Subsequently, the specimens were placed in oedometers and vertical stresses of 25 kPa, 50 kPa, 100 kPa, 200 kPa, 400 kPa, 800 kPa were applied successively. Before applying the next level of vertical stress, it is necessary for the vertical deformation rate to be less than 0.01 mm per hour.

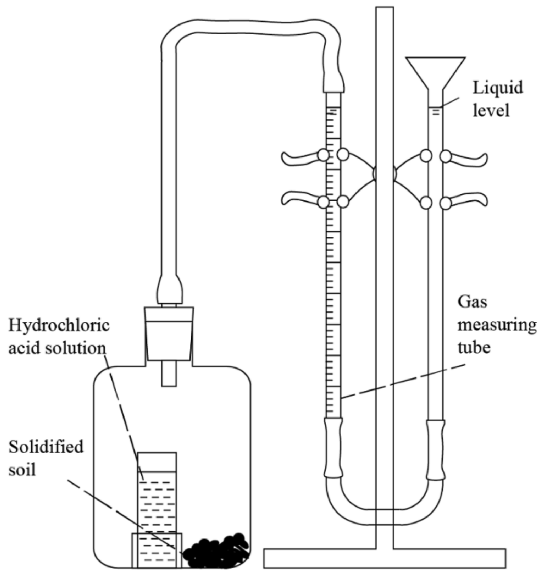

Fig. 2. Sketch diagram of the carbonates measuring apparatus.

To investigate the CO_2 mineralization, the quantity of carbonates was measured by acid digestion through a self-assembled glass gas burette. As shown in Fig. 2, the oven-dried powder of the carbonated specimen was weighed and placed in the flask. Hydrochloric acid solution consisting of one volume of hydrochloric acid mixed with three volumes of water was placed in the flat-bottomed test tube. The measuring tubes in the right of the schematic diagram were filled with mixture solution of sulfuric acid and methyl red to facilitate the observation of gas volume changes. Before testing, the apparatus was properly assembled ensuring that it was well air-tight. Then, the two liquid levels in the measuring tubes were adjusted to be consistent. The hydrochloric acid and specimen powder were mixed and reacted sufficiently at 25 °C and 1 atm after the tilt and shake of flask. As reaction continued, a difference occurred between the two liquid levels due to the pressure, and both liquid levels became stable. Therefore, the CO_2 mineralization was calculated from the value difference before and after the left measuring tube, after the liquid levels in the left and right were adjusted to be consistent again.

To investigate the chemical effect of TEA on the soil-binder-CO_2 system, the pH of binder pastes and zeta potential were tested. Eco-binder with 60 % GGBS, 20 % CCR and 20 % MK was mixed with specific TEA solution to form the eco-binder paste with a W/C of 0.6 in a flask. The mixture was stirred by magnetic stirrer continuously. At designated time point (30 min, 15 min, 60 min, 240 min and 480 min), the paste was placed into centrifugal tube and centrifuged at 3000 r/min for 10 min. The liquid supernatant was filtered through a filter membrane of 0.22 μm, and the pH value was detected with a pH meter. The zeta potential of carbonated soil was measured by Malvern-Zetasizer Nano S90 (UK).

3. Results and discussion

The UCS, CO_2 mineralization and CE of specimens with 1.5 % TEA and 10 wt% binders of varying constituent ratio all increase with carbonation age, as shown in Fig. 3. The UCS is significantly influenced by the binder constituent ratio, showing an obvious unimodal form. With the increase of carbonation age, the optimal ratio of MK: GGBS: CCR based on UCS moves from about 3:5:2 to 2:3:5, indicating that the strength growth of carbonated specimen needs more

CCR with the extension of carbonation age. The highest UCS of specimens subjected to a 1-d carbonation is about 3 MPa, while after a 7-d carbonation, the value is up to 4.45 MPa. The UCS of 10P1.5T6G2C2K-M7 is 49 % higher than 10P1.5T6G2C2K-M1. Benefitted from the high content of aluminum in MK and the promotion of aluminum dissolution by TEA, the generation of the binding phase C-(A)-S-H and ettringite has been promoted. Overall, the addition of MK increases the UCS of carbonated specimen through filler effect and the reaction mentioned above.

Under 25 °C and 1 atm, the CO_2 mineralization can be calculated according to

$$m_{cr} = \frac{V}{V_m} \times \frac{1000}{m_s} \times M_{CO_2} \quad (1)$$

where m_{cr} denotes the CO_2 mineralization (g) per kilogram

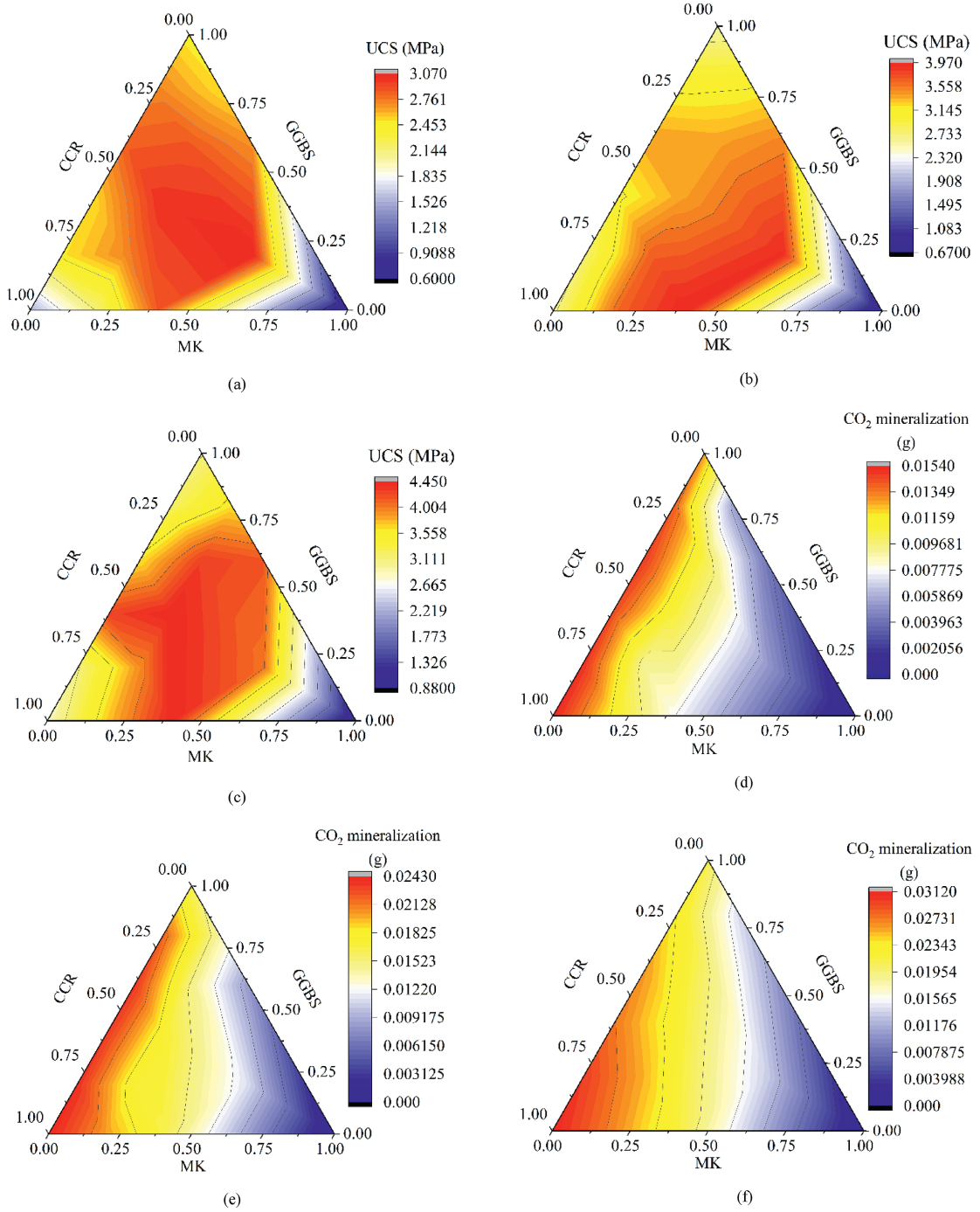

Fig. 3. The UCS and CO_2 mineralization of specimens with different constituent ratios. (a) UCS of specimens with different binder ratios carbonated for 1 d; (b) UCS of specimens with different binder ratios carbonated for 3 d; (c) UCS of specimens with different binder ratios carbonated for 7 d; (d) CO_2 mineralization of specimens with different binder ratios carbonated for 1 d; (e) CO_2 mineralization of specimens with different binder ratios carbonated for 3 d; (f) CO_2 mineralization of specimens with different binder ratios carbonated for 7 d; (g) CE of specimens with different binder ratios carbonated for 1 d; (h) CE of specimens with different binder ratios carbonated for 3 d; and (i) CE of specimens with different binder ratios carbonated for 7 d.

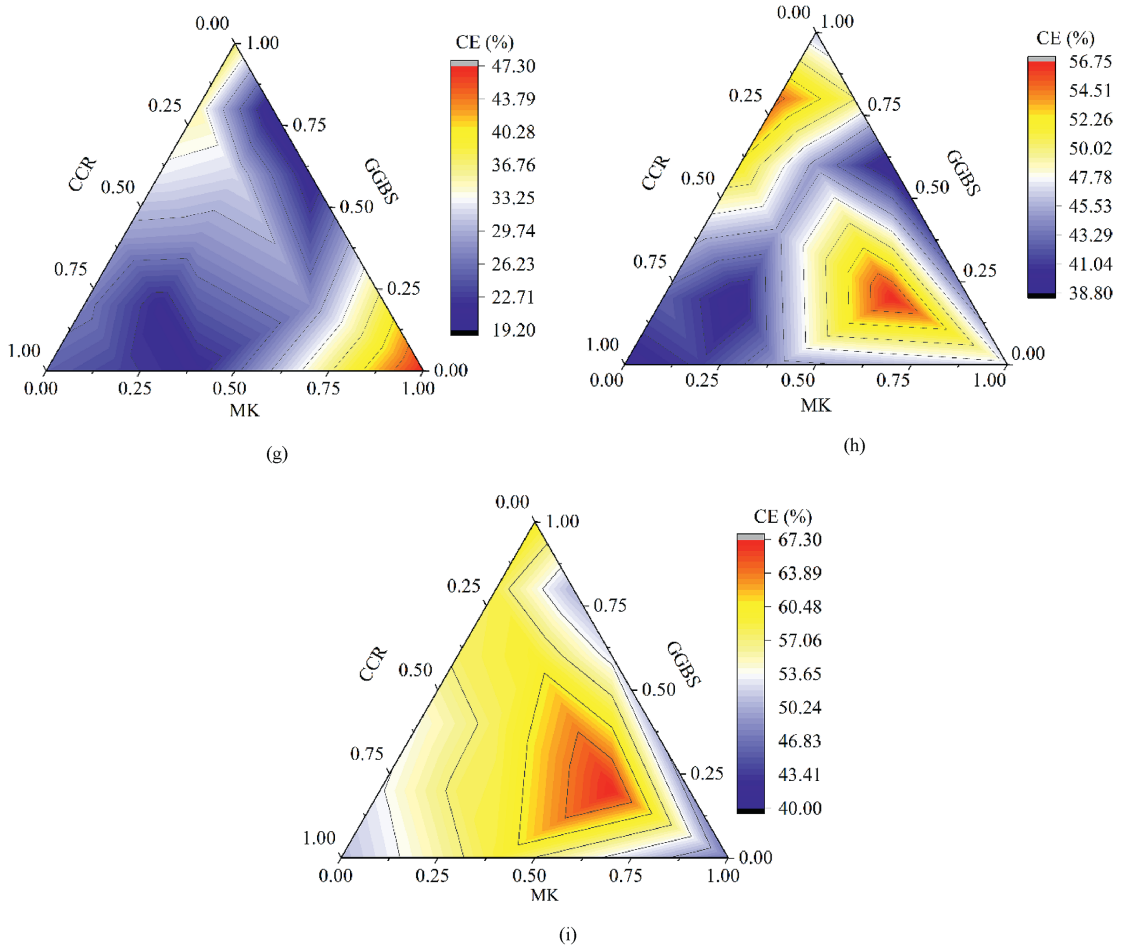

Fig. 3. (*continued*).

carbonated soil, V is the CO_2 gas volume read by gas measuring tube, V_m indicates the molar volume (24.5 L/mol, 25 °C, 1 atm), M_{CO_2} is the molar mass of CO_2, and m_s is the mass (g) of specimen weighed.

To distinguish the efficiency of CO_2 mineralization caused by the TEA addition, CE is defined as Eq. (2).

$$CE = \frac{m_{cr}}{m_{cp}} \tag{2}$$

where m_{cp} is the mass (g) of potential CO_2 mineralization per kg carbonated soil calculated from the calcium and magnesium content in the binders.

The CO_2 mineralization of carbonated specimens decreases in a ladder pattern with increasing MK content, due to the low calcium content of MK. The CO_2 mineralization remains relatively low when the ratio of CCR in the binder does not exceed 20 %. For specimens carbonated for 7 d, the highest CO_2 mineralization occurs in the binders consisting solely of CCR, due to the high calcium concentration and pH value in the soil pore water. The CO_2 mineralization of 10P1.5T6G2CK-M increases by 87.8 % from 1-d to 7-d carbonation, significantly surpassing its UCS. The plot of CE changes from a saddle form at the early carbonation stage into a unimodal form after 7-d carbonation. The CE grows almost constantly with the increase of MK, facilitating more efficient calcium utilization, in accordance with what was reported by Bernal et al. (2010). Except for the specimens with high MK content, a higher CE is exhibited in specimen with a CCR to GGBS ratio of about 1:1, reaching up to 67.3 % specifically for 10P1.5T3G3C4K-M7. As carbonation age increases, the calcium ions in the specimen with high CCR and GGBS content are gradually consumed by the carbonate and bicarbonate ion, resulting in the CE peak movement. The destruction of Al-O bind results in the release of $Al(OH)_6^{3-}$ or $H_3AlO_4^{2-}$ (Li et al., 2022). Given that MK is the primary Al-bearing material, the relatively efficient chelation of TEA with aluminum in MK provides reactants for the aluminum reaction. As Al^{3+} dissolves from MK, the aluminate reaction is accelerated during early hydration (Huang et al., 2021).

The UCS and CE of the specimens solidified with varying contents of binders consisting of 60 % GGBS, 20 % CCR and 20 % MK, are presented in Fig. 4. With the increase of binder content, CE reduces slightly after reaching peak at binder content of 10 %. The lower CE of specimens with binder content of 5 % can be attributed to the low alkalinity of the pore water. The reduction of CE after peak is relevant to the incomplete carbonation reaction, that is, the binder that has not been carbonated still exists after 7-d carbonation. Specimens with a TEA dosage of 1.5 % showed a significant enhancement in CO_2 mineralization by approximately 2.2 times, compared to those without TEA. The binder content corresponding to the peak of CE increases due to the addition of TEA. Therefore, the addition of TEA obviously promotes the sufficient consumption of calcium and magnesium by carbonates thereby stimulates the carbon sequestration potential of soft soil solidified with eco-binder.

As demonstrated in Fig. 4, the UCS of 10P1.5T6G2C2K is

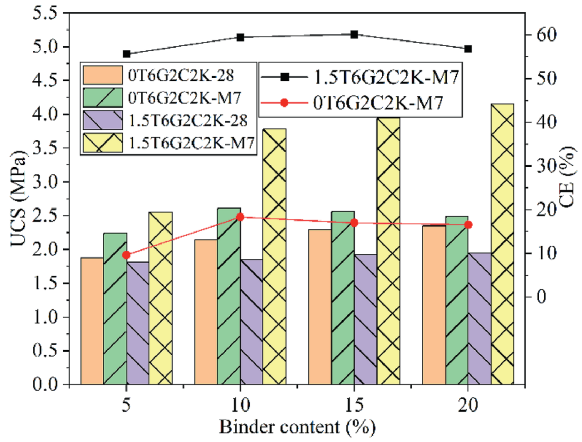

Fig. 4. UCS and carbonation efficiency of specimens with different binder contents.

increased by 104 % through carbonation, indicating the reinforcing effect of the carbonates on the structure of solidified soft soil. The UCS of specimen increases gradually with binder content, except for the carbonated specimens without TEA. The UCS growth rate of carbonated specimens with 1.5 % TEA is significantly higher than that of the other three groups, suggesting that the increased binder is fully reacted under TEA and carbonation to produce the strength-enhancing products. Comparing carbonated specimens with and without TEA, it can be concluded that the addition of 1.5 % TEA further enhances the UCS of solidified soft soil for 13.84 %–66.59 %. It is noteworthy that the uncarbonated specimens with 1.5 % TEA exhibit significantly lower strength compared to those without TEA. This can be attributed to the formation of a hydration-retarding TEA-cation complexion layer and the adsorption onto the CH surface of TEA (Zhang et al., 2016). Addition of high dosage TEA harms the products from hydration and pozzolanic reactions. Thus, it can be inferred that there is a synergistic effect between the addition of TEA and carbonation on the reinforcement of soft soil by eco-binder.

Fig. 5 demonstrates the UCS and CE of the specimen with various TEA dosages. Each group of different curing regimes shows a trend of initial increase and then decrease with increasing TEA dosage. As carbonation age goes up, the optimal TEA dosage corresponding to the peak UCS increases. The UCS of specimens with 5 % TEA are quite lower than the other groups, which indicates an excessive addition of TEA causes distinct decline in the strength of carbonated soft soil solidified with the eco-binder. For the specimens carbonated for 1 d, the optimal TEA dosage tested is 0.15 %, while that for specimens carbonated for 7 d is around 1.5 %. Results suggest that the generated carbonates counteract the detrimental effects of TEA on the solidified soil.

Different from the trend of strength, CE increases with TEA dosage continuously, illustrating that the addition of TEA has a stable enhancement on the carbonation of eco-binder. Therefore, the reduction of the carbonates is not the reason why the UCS decreases. Noting the growth rate of CE slowed down with TEA dosage, and the optimal TEA dosage is 1.5 % considering the trend of UCS.

As shown in Fig. 6, the compaction curve of plain soft soil is generally lower than that of soil solidified by eco-binder with different TEA dosages. Therefore, it can be concluded that within the test range, the water content decreased with TEA dosage. As for the maximum dry density, solidified soft soil with 1.5 % TEA exhibits a higher maximum dry density compared to that with 5 % TEA and to the soil without TEA. It can also be understood that the

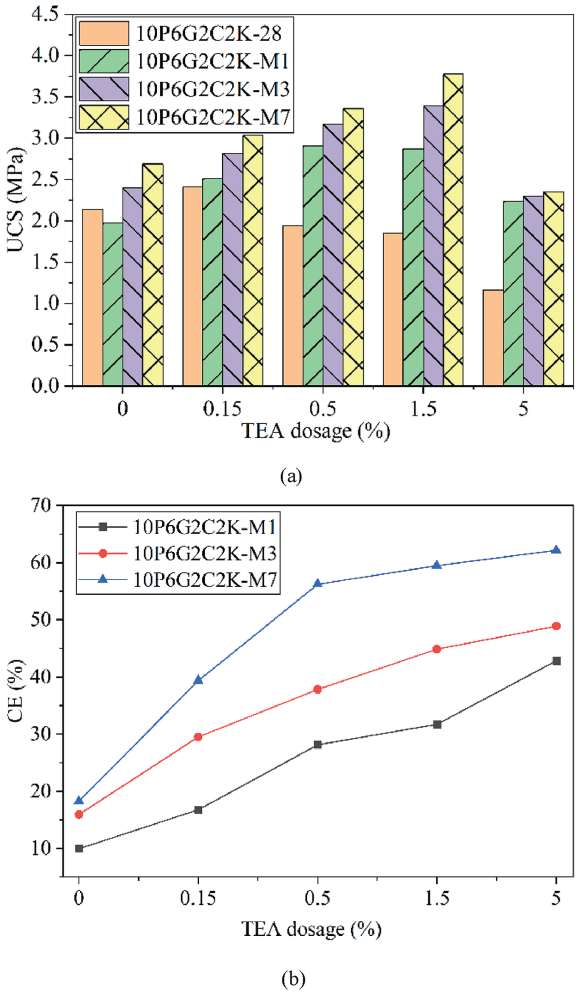

Fig. 5. UCS and carbonation efficiency of specimen with various TEA dosages. (a) UCS of soil specimens with various TEA dosage and curing time; and (b) CE of soil specimens with various TEA dosage and curing time.

appropriate addition of TEA makes the solidified soil achieve a higher dry density of the same water content. Due to the increased dry density, the strength of solidified soil is thus improved.

The compression curves of the soft soil with different treatment regimens can be seen from Fig. 7. It is worth to be noticed

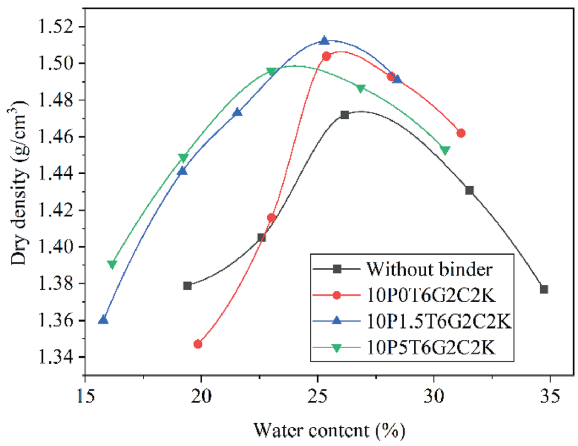

Fig. 6. Compaction curves of the carbonated soil with different TEA dosages.

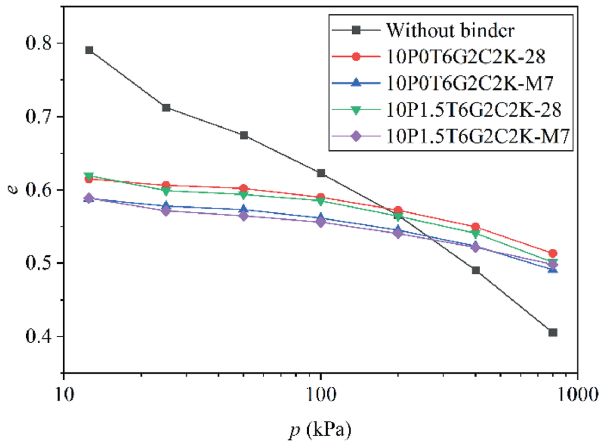

Fig. 7. Compression curves of the carbonated soil with different TEA dosages.

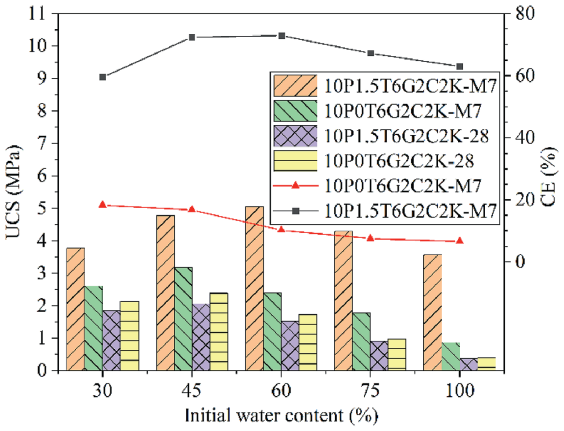

Fig. 8. UCS and CE of specimens with different initial water contents.

that there are differences in the initial porosity (e_0) of specimens, which can be attributed to the different mineral compositions of soils undergone different treatments, resulting in the different specific gravities. To quantify the compressibility characters of soil, the coefficient of compressibility (α_v, 0.1–0.2 MPa) can be calculated from the curves, and the results are shown in Table 3. The soil without the reinforcement of eco-binder has an α_v of 0.352 MPa^{-1}, which can be attributed to the incorporation of 10 % sand. As a contrast, α_v of 10P0T6G2C2K-M7 are generally lower than 1/3 of that of the plain soil. As shown in Table 3, the carbonated soil has a greater compressibility character, comparing to that of the uncarbonated soils with the same TEA dosage. The carbonated soil with 1.5 % TEA has the lowest α_v, while the α_v of uncarbonated soil with 1.5 % TEA is higher for about 33 %. However, for the uncarbonated soil, the α_v of 10P1.5T6G2C2K-M7 is higher by 19.8 % than that of 10P0T6G2C2K-M7, indicating that the addition of 1.5 % TEA increased the compressibility of the solidified soil. The addition of 1.5 % TEA offsets a part of the enhancement effect of the solidification on the soil rigidity. Nevertheless, TEA addition has no obvious negative effect on the compressibility of carbonated specimens.

The UCS and CE of specimens with different initial water contents are shown in Fig. 8. For each group, the UCS shows a trend of increase first following a decrease with water content. The optimal water content for the strength development is around 45 %, except for 10P1.5T6G2C2K-M7 of which the optimal water content is around 60 %. The initial water content is a significant factor on the hydration and carbonation of the eco-binder in soft soil.

Due to the fact that the carbonation reaction depends on the CO_2 gas diffusion (Li et al., 2023c), the poor permeability of clay soil leads to a generally low carbonation efficiency which differs from carbonated specimen with TEA. For the carbonated specimen without TEA, the excess initial water occupies the inflow channel of CO_2, and retards the carbonation reaction in return. On the other hand, the excess water increases the porosity of soil and reduces the soil internal friction and cohesion. Among the test groups of specimens, the highest UCS corresponds to the 10P1.5T6G2C2KM with a water content of 60 %. The addition of 1.5 % TEA increases the optimal initial water content, which could be associated with the more efficient carbonation reaction. In 10P1.5T6G2C2K-M7 more water was required, in order to produce more hydration products. Although the excess initial water occupies the soil pores, the increase in the solubility of CO_2, as a consequence of the TEA, serves to avoid the hindrance of carbonation. But as the initial water content rose from 60 % to 100 %, both CE and the UCS inevitably decrease.

The leaching of ions from GGBS, CCR and MK are accompanied by the changes in the pH of pore solution. The pH of the binder pastes before the carbonation is shown in Fig. 9, and can reflect the pore solution of solidified soil. A high pH value indicates a great carbonation reactivity. The addition of TEA distinctly elevates the alkalinity of the paste solution, due to the calcium chelation of TEA, and thus accelerates the dissolution of calcium hydroxide and the calcium oxide. The pH value increases with time at the beginning of mixing. Except for the paste with 5 % TEA, the peak pH appears around the mixing time of 60 min. The fluctuation in pH after reaching peak stems from the consumption of CH through pozzolanic reaction, yielding results similar to those of Jiang et al. (2024). The elevated pH of paste contributes to the absorption and ionization of CO_2, and the formation of calcium carbonate. Note that the pH of pastes increases with TEA dosage after 60-min mixing, indicating one of the reasons for the positive effect of TEA on the soil carbonation efficiency.

The zeta potential of 10P6G6C6K-M7 with different TEA dosages is shown in Fig. 10. The zeta potential reflects the dispersion of solidified soil particles and the carbonation products. Because of the negative charge on the soil particle surface caused by the cation exchange, the solidified soil exhibits a negative zeta potential. The carbonated soil specimens always show a negative Zeta potential. And the surface of calcium carbonates has positive charge. As TEA dosage increases, the absolute value of Zeta potential of the carbonated soil decreases continuously, reducing the repulsive force between particles solidified soil after 7 d carbonation, and enhancing the particle aggregation. Although the zeta potential increases slightly after the TEA dosage of 1.5 %, further marginal addition of TEA inhibits the nucleation of the C-S-H of which surface is charged negatively (Jiang et al., 2024), and thus leads to the increase of negative zeta potential.

Table 3
Coefficient of compressibility of tested specimens.

Specimen	Plain soil	10P0T6G2C2K-28	10P0T6G2C2K-M7	10P1.5T6G2C2K-28	10P1.5T6G2C2K-M7
α_v (MPa^{-1})	0.352	0.111	0.104	0.133	0.100

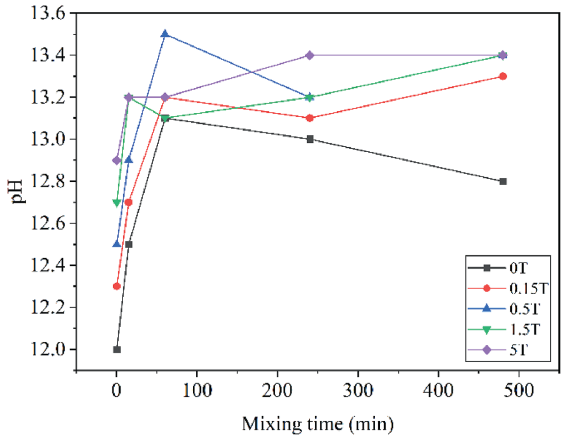

Fig. 9. The pH values of binder pastes with various TEA dosages.

The microscopic images of the carbonated soil specimens are shown in Fig. 11. As shown in Fig. 11a and b, rhombohedral calcite, spindle-needle shaped aragonite and spherical vaterite could be observed in 10P1.5T6G2C2K-M7 as the polymorphs of calcium carbonates. In the inter-particle pores, the needle shaped aragonites aggregate to form carbonates clusters, which results in the denser particle structure. The pores-filling effect and the particle-cementing effect of polymorphs of $CaCO_3$ crystals play important roles on the strength growth of carbonated soil. And the appropriate addition of TEA accelerates the leaching of Ca^{2+}, and thus promotes the crystallization of $CaCO_3$ as well generates C-S-H that cements fine particles into aggregates. Comparing with specimens of other groups, the 10P1.5T6G2C2K-M7 has denser structure. Notably, the flaky clay particles aggregated together in 10P1.5T6G2C2K-M7, indicating an aggregation effect of TEA on soil, which is consistent with the results of zeta potential. The modification of the clay surface by TEA leading to the creation of surface charge could be one reason for this effect, as reported in recent studies (Elkhalifah et al., 2013; Godarziani et al., 2022).

Regarding the carbonated specimen without TEA, calcium carbonates (calcite and aragonite) and acicular ettringite could be observed in Fig. 11c and d. Distinct crystalline calcite is absent from the field of view. Instead, the aragonite and vaterite are the major form of carbonation products, which has a weaker pore filling effect than calcite. As shown in Fig. 11e and f, the hydration products (C-S-H and ettringite) were not found throughout the visual field of 10P5T6G2C2K-M7, which confirms the negative effect of TEA on the C-S-H nucleation as described above. The aragonite and small

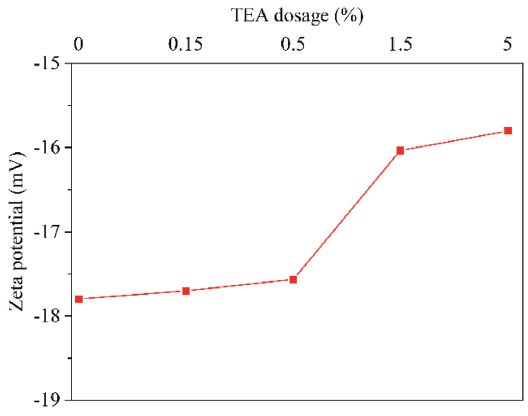

Fig. 10. Zeta potential of carbonated soil with various TEA dosage.

crystalline calcite accounts for large proportion of the carbonation products phase of the 10P5T6G2C2K-M7, according to the SEM image. What is particularly notable in this SEM image is the higher porosity of 10P5T6G2C2K-M7 than the other carbonated soil with different TEA dosages. Therefore, the negative effect of high TEA dosage on the strength of carbonated soil is related to the degeneration of hydration products and the increase in porosity caused by the transformation of carbonates polymorphs.

To distinguish the effect of high initial water content on the soil carbonation, the SEM images of 1.5T10P6G2C2K-M7 (with initial water content of 60 %) are shown in Fig. 11g–h. In contrast to the specimen with initial water content of 30 %, the SEM reveals the well-developed calcite and C-S-H gel, suggesting a more adequate hydration and carbonation reaction, which is consistent with the results of UCS and CE. Spherical vaterite, meanwhile, can be observed in the fine pores between the soil particles.

Fig. 12 presents the XRD patterns of solidified specimens after 7-d carbonation. To amplify the acceleration of carbonation caused by triethanolamine, the specimens selected here were with a triethanolamine of 5 %, and with no MK added. As shown in Fig. 12, the calcite and quartz are the major minerals in the carbonated soil, and aragonite and vaterite were also detected. Other clay minerals were not distinguished here. The enhancement of calcite diffraction peak with binder content can be identified from Fig. 12, providing explanation for the UCS and CE results above. For the 10P0T6G4C0K-M7, the diffraction peaks of calcite and aragonite are weaker than that of 10P5T6G4C0K-M7, suggesting a poor carbonation in the specimens without TEA.

Fig. 13 presents the TGA patterns of carbonated soil with different binder contents and TEA dosages. According to the curves of derivative weight loss, the weight loss peaks ranging of 30 °C–150 °C, 200 °C–300 °C, 400 °C–500 °C and 550 °C–850 °C, correspond to the dehydration of clay minerals, the dehydration of ettringite and C-S-H, the dehydration of CH and the decomposition of calcium carbonates, respectively. TEA evaporation can be regarded as between the temperature from 300 °C to 650 °C. With the binder content, the weight loss of calcium carbonates elevates from 2.76 % to 6.86 %. Regarding the binder content, the calcium carbonates formation efficiency of specimen with 20 % binder content is lower than that of 5 % binder content, suggesting the limitation of carbonation under the addition of 5 % TEA may be related to the initial water content. And the weight loss of 10P1.5T6G4C0K-M7 between 550 °C and 850 °C is about 3.56 %, lower than that of 4.45 % with 5 % TEA dosage. Whereas the total weight loss of 10P1.5T6G4C0K-M7 is similar to 10P5T6G4C0K-M7, and thus the hydration products in 10P1.5T6G4C0K-M7 is more than 10P5T6G4C0K-M7, confirming the instability of C-S-H and CH in high concentration TEA.

4. Discussion

As stated above, the addition of TEA promoted the carbonation reaction in the soft soil, and thus reinforced the solidified soft soil. The application of TEA in the carbonation-solidification of soil also avoids high-pressure ventilation and reduces the use of caustic alkalis, which may pose harm to the soil and water environments. Due to the low dosage and the biodegradation of TEA (Qiu et al., 2024; West and Gonsior, 1996), environmental risks do not hinder the application of TEA in the carbonation-solidification of soil. As shown in Fig. 14a, the carbonation promotion caused by TEA can be divided into three parts: ion dissolution, CO_2 capture and carbonates precipitation, sequentially. Each of the above three parts was proved to be the controlling factor of the carbonation reactions (Wang et al., 2019c). The concentration of Ca^{2+} and the alkalinity of the pore water in the binder-soil system are caused by

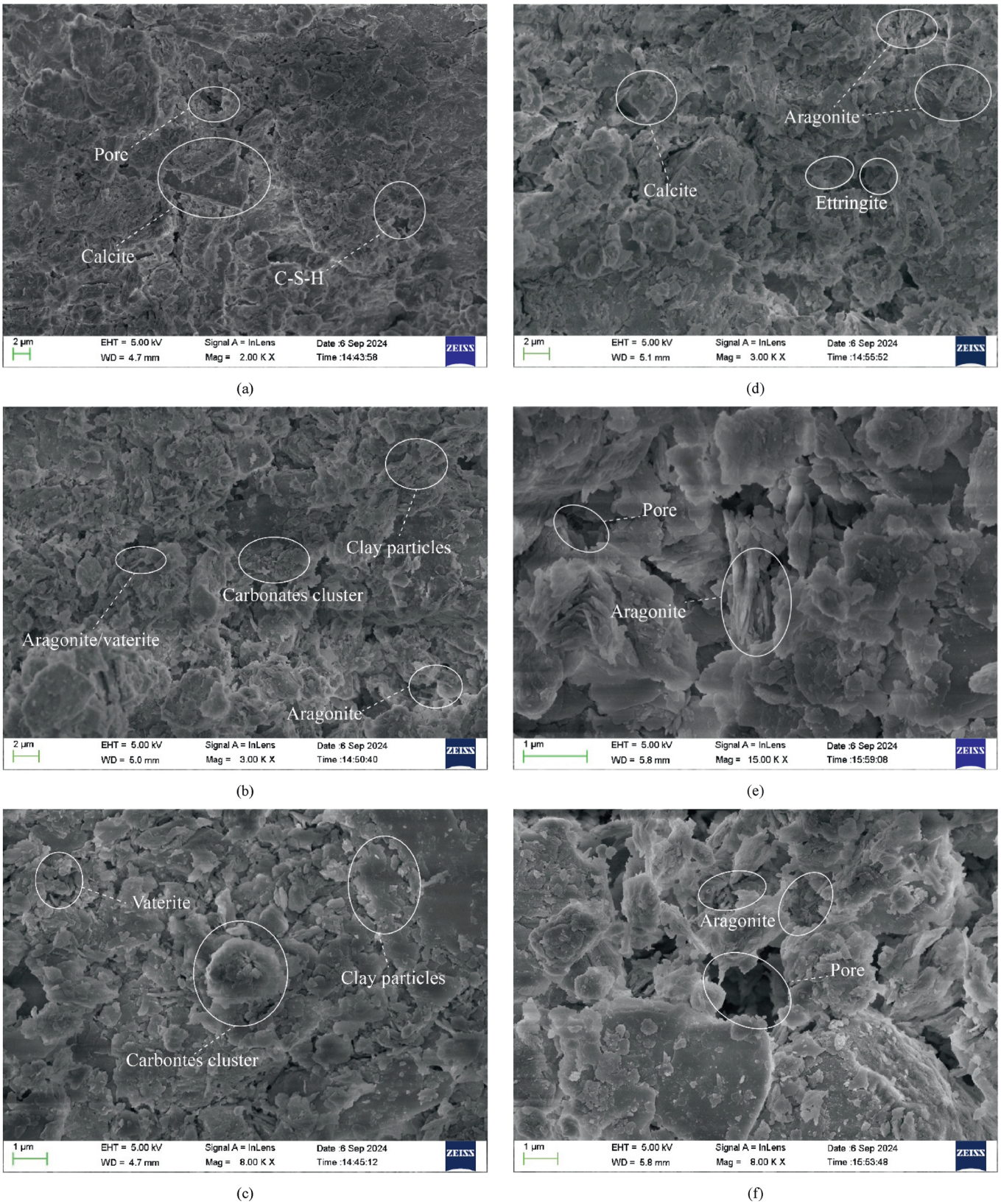

Fig. 11. SEM images of carbonated soil with various TEA dosage. (a) The microstructure of 10P1.5T6G2C2K-M7; (b) The calcium carbonates filling in the pores; (c) The microstructure of 10P0T6G2C2K-M7; (d) Carbonates and hydration production in 0T10P6G2C2K-M7; (e) Aragonite clusters in the pores of 10P5T6G2C2K-M7; (f) The microstructure of 10P5T6G2C2K-M7; (g) The microstructure of 1.5T10P6G2C2K-M7 (60 % initial water content); and (h) Soil particles bonded by C-S-H.

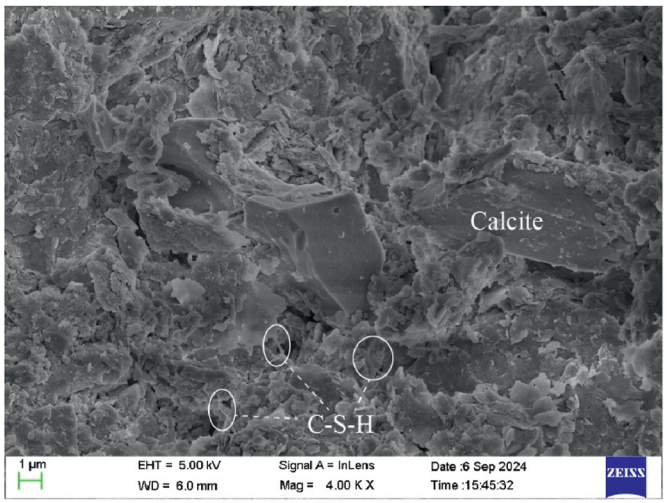

(g)

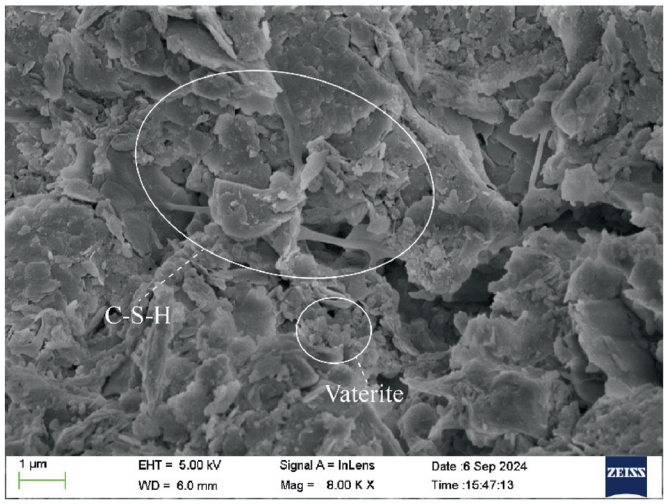

(h)

Fig. 11. (*continued*).

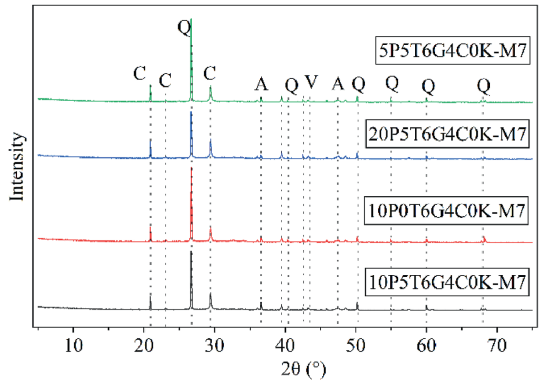

Fig. 12. XRD patterns of carbonated soil solidified with eco-binders (A: Aragonite, C: Calcite, Q: Quartz, V: Vaterite).

the chelation of TEA. Besides, due to the promoted dissolution, the appropriate addition of MK showed an enhancement on the strength growth.

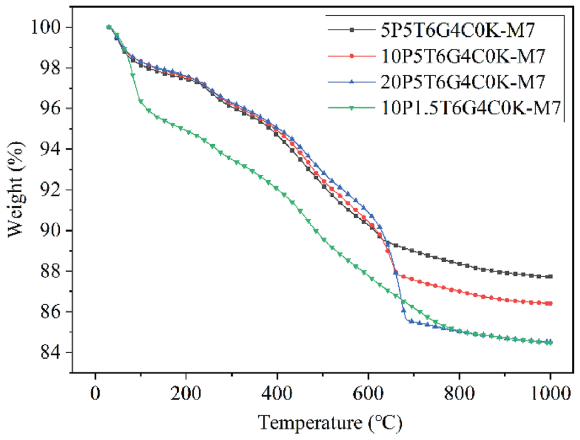

(a)

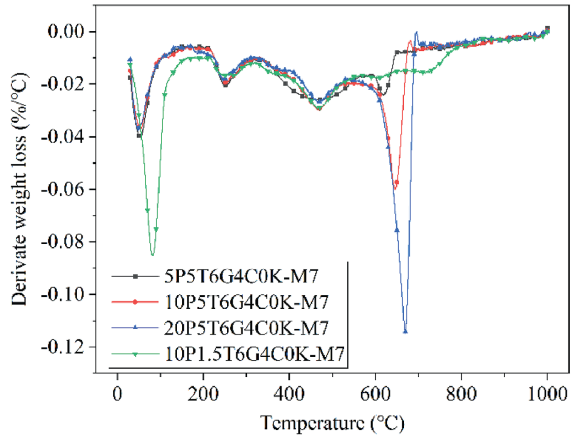

(b)

Fig. 13. TGA patterns of carbonated soil solidified with eco-binders. (a) Variations in the weight of carbonated specimens; and (b) derivative thermogravimetric curves of carbonated specimens.

TEA acts as a catalyst in the hydrolysis of CO_2 via the following reactions (Eqs. (3) and (4)), and thus promotes the dissolution of $Ca(OH)_2$. Due to the catalytic effect of TEA on CO_2 dissolution, the addition of TEA increases the solubility of CO_2 in the soil pore solution. Therefore, the CO_2 in the atmosphere transfers into solution phase, during the carbonation curing, and the absorption was promoted by the increase of TEA dosage. However, the excessive addition of TEA impacted adversely on the strength growth by the adsorption on the hydration products. Precipitation is facilitated due to the more carbonate and calcium ions dissolved in pore solution, and thus the pore structure was densified.

$$H_2O + R_3N \rightleftharpoons OH^- + R_3NH^+ \quad (3)$$

$$OH^- + CO_2 \rightleftharpoons HCO_3^- \quad (4)$$

Based on the existing test results from the other previous studies, the CE and UCS of different types of solidified soil under various carbonation conditions are listed on Table 4 (Cai and Liu, 2017; Phan et al., 2017; Yi et al., 2016; Wang et al., 2019c, 2024, 2025; Yu et al., 2021, 2022). The present study avoided the high-pressure ventilation and high-purity CO_2 gas, thus making it more feasible to the conduction of solidified soft soil carbonation.

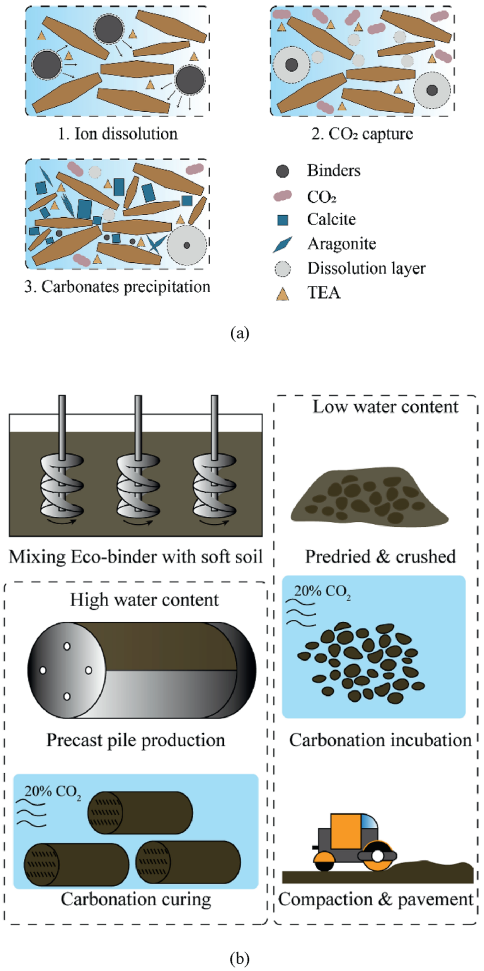

Fig. 14. The application and application of TEA-accelerated soil carbonation. (a) Reinforcement mechanism diagram of eco-binder solidified soil with TEA subjected to carbonation; and (b) the application scenarios of the eco-binder solidified soil with TEA subjected to carbonation.

Although the carbonation conditions are relatively mild, the CE and the strength growth brought by carbonation are still at a relatively high level compared with previous studies.

Although the TEA has been clarified to promote carbonation in soft soil solidified with eco-binder, problems such as TEA recycling, kinetic models of eco-binder carbonation and large-scale application are still to be addressed. In existing practices, the carbonation was used to recycling soft soil and alkaline IBPs by injecting high-pressure CO_2 through perforated pipes (Liu et al., 2021b). Whereas for the carbonation conducted in ambient pressure, the solidified soil can be applied in substituting concrete blocks, restoration of monuments and contaminated site remediation, etc. In this study, the potential application scenarios of carbonation with the catalyst of TEA includes carbonation curing of precast pile, direct mixing of TEA solution saturated with CO_2, or, carbonation before compaction.

5. Conclusions

Above all, the mechanism of the reinforcement and CO_2 mineralization of carbonated soil solidified with metakaolin was investigated in this study. The effects of binder content, binder constituent, initial water content and TEA dosage on the carbonation and reinforcement of solidified soil were investigated. The mineral phase and soil structure influenced by TEA and carbonation were clarified. The conclusions drawn from this study are as follows:

(1) The optimal ratio of GGBS:CCR:MK for carbonation-solidification is 4:4:2. The incorporation of MK promotes the carbonation and hydration of the mixed ternary binder. GGBS and CCR provides an alkaline environment for the solidified soil system and calcium ions required for carbonation reaction. Besides, the GGBS introduces the necessary silicon components ensuring the formation of bonding C-S-H.

(2) The carbonation efficiency and strength of carbonated specimen with 1.5 % TEA were higher. Due to the occupation of CO_2 inflow channel and the insufficient reactant for hydration and ion dissolution, the optimal initial water content for carbonated soil with TEA was tested to be around 60 %, while that of the carbonated soil without TEA is lower, indicating that the addition of TEA increases the CO_2 solubility and carbonation. By promoting ion dissolution from binder, increasing binder-water system alkalinity and CO_2 dissolution, the CO_2 mineralization of carbonated specimen increased constantly with TEA dosage. For specimen solidified with 10 % binder (GGBS:CCR:MK = 4:4:2), the CO_2 mineralization of specimen with 1.5 % TEA was tested to be 3.2 times of that without TEA.

(3) The addition of 1.5 % TEA elevated the maximum dry density of soil solidified with 10 % binder from ~1.50 to ~1.52 (g/cm^3), and reduced the optimal water content for >1 %. The addition of 1.5 % TEA has no obvious impact on the compressibility of carbonated soil. But the coefficient of compressibility of solidified soil with TEA subjected to

Table 4
CE and UCS of carbonated soils under various carbonation conditions (P: carbonation pressure, w_0: water content, T: temperature, t: carbonation time).

Soil	Additive	Carbonation condition						*CE* (%)	*UCS* (MPa)	Reference
		P (kPa)	w_0 (%)	*T* (°C)	*c* (%)	*RH* (%)	*t* (h)			
Sediment	20 %MgO-based binder	–	70	–	99.9	98	24	72.5	–	Phan et al. (2017)
Sludge	10 %MgO 1 %$MgCl_2$	50	28	20	20	70	168	33.45	5.07	Wang et al. (2024)
Kaolin clay	8 %MgO 12 %FA	150	17	22	99.9	–	24	66.0	–	Wang et al. (2019c)
76.9 % Sludge 23.1 % Sand	5 %MgO 5 %GGBS	150	15	–	99.9	–	12	71.6	1.9	Wang et al. (2025)
Low-liquid limit silt	20 %MgO	200	25	22	99.9	–	6	82.91	2.5	Cai and Liu (2017)
Quartz powder	30 %SS	200	18	–	99.9	–	18	22.23	~1.5	Yu et al. (2021)
Quartz powder with 20 % montmorillonite	30 %SS	200	18	–	99.9	–	6	53.45	0.76	Yu et al. (2022)
Lean clay	15 %MgO	200	25	–	99.9	–	12	81.87	~2.5	Yi et al. (2016)

carbonation was 24.8 % lower than uncarbonated solidified soil.

(4) Due to the accelerated carbonation and the optimized compaction, the peak UCS of carbonated specimen is observed at the TEA dosage of approximately 1.5 %. The peak UCS increased for 66.6 % and the strength of carbonated specimen with 5 % TEA was decreased, compared to those without TEA specimen. For the uncarbonated specimen, the strength enhancement only occurred at the TEA dosage of 0.15 %, and the strength was lower than that without TEA when the TEA dosage is higher than 0.5 %, which was related to the nucleation hindering and adsorption effect of TEA on the hydration products. The carbonation offsets the adverse effect of TEA on the strength growth of solidified soil. Thus, the synergistic effect of TEA and carbonation further reinforces the solidified soil.

(5) The calcium carbonates polymorphs (calcite, aragonite, vaterite) were the strength-determining mineral phase in the carbonated soil with TEA, through pores filling and particle cementing. The addition of TEA promotes the generation of calcium carbonates. The carbonates tend to exist in the form of calcite in the low TEA dosage, and it turns out to be more aragonites clusters in the carbonated soil with higher TEA dosage. The absolute value of zeta potential of carbonated soil decreases due to the addition of TEA, and result in the enhancement of soil particle aggregation. The carbonated soil with 1.5 % TEA has a denser particle structure than that with 5 % TEA.

CRediT authorship contribution statement

Zhuoyu Duan: Writing – review & editing, Writing – original draft, Validation, Project administration, Methodology, Investigation, Formal analysis, Data curation, Conceptualization. **Dongxing Wang:** Writing – review & editing, Supervision, Funding acquisition, Conceptualization. **Yong Zou:** Writing – review & editing, Supervision. **Hao Luo:** Writing – review & editing, Visualization, Formal analysis.

Declaration of competing interest

The authors declare that they have no known competing financial interests or personal relationships that could have appeared to influence the work reported in this paper.

Acknowledgments

This work was supported by the National Natural Science Foundation of China (Grant No. U24A20183), Science Fund for Distinguished Young Scholars of Hubei Province (Grant No. 2024AFA051) and Youth Science Fund (A-class) of Hunan Natural Science Foundation (Grant No. 2025JJ20049).

List of symbols

α_v	Coefficient of compressibility
CCR	Calcium carbide residue
CE	Carbonation efficiency
CH	Calcium hydroxide
C-S-H	Calcium silicate hydrate
GGBS	Ground granulated blast-furnace slag
MK	Metakaolin
TEA	Triethanolamine

References

ASTM D4318-17e1, 2018. Standard Test Methods for Liquid Limit, Plastic Limit, and Plasticity Index of Soils. ASTM International, West Conshohocken, USA. https://doi.org/10.1520/D4318-17E01.

ASTM D7928-21e1, 2021. Standard Test Method for Particle-Size Distribution (Gradation) of Fine-Grained Soils Using the Sedimentation (Hydrometer) Analysis. ASTM International, West Conshohocken, USA. https://doi.org/10.1520/D7928-21E01.

Ben, X.Q., Jiang, L.H., Ji, C.W., Jin, W.Z., Chen, L., Zhi, F.F., Yang, G.H., 2024. Effect of triethanolamine on cement paste exposed to external sulfate attack. Constr. Build. Mater. 411, 134755. https://doi.org/10.1016/j.conbuildmat.2023.134755.

Bernal, S.A., De Gutierrez, R.M., Provis, J.L., Rose, V., 2010. Effect of silicate modulus and metakaolin incorporation on the carbonation of alkali silicate-activated slags. Cement Concr. Res. 40, 898–907. https://doi.org/10.1016/j.cemconres.2010.02.003.

Cai, G.H., Liu, S.Y., 2017. Compaction and mechanical characteristics and stabilization mechanism of carbonated reactive MgO-stabilized silt. KSCE J. Civ. Eng. 21, 2641–2654. https://doi.org/10.1007/s12205-017-1145-1.

Chen, T.F., Gao, X.J., Qin, L., 2019. Mathematical modeling of accelerated carbonation curing of Portland cement paste at early age. Cement Concr. Res. 120, 187–197. https://doi.org/10.1016/j.cemconres.2019.03.025.

Elkhalifah, AliE.I., Maitra, S., Bustam, M.A., Murugesan, T., 2013. Effects of exchanged ammonium cations on structure characteristics and CO_2 adsorption capacities of bentonite clay. Appl. Clay Sci. 83, 391–398. https://doi.org/10.1016/j.clay.2013.07.016, 84.

Godarziani, H., Ramezanipour Penchah, H., Ghaemi, A., 2022. Triethanolamine-modified montmorillonite clay as a new adsorbent for CO_2 capture: characterization, adsorption, and RSM modeling. J. Chin. Chem. Soc. 69, 1981–1996. https://doi.org/10.1002/jccs.202200395.

Han, S.H., Jun, Y.B., Kim, J.H., 2023. The use of monoethanolamine CO_2 solvent for the CO_2 curing of cement-based materials. Sustain. Mater. Technol. 35, e00559. https://doi.org/10.1016/j.susmat.2022.e00559.

Heren, Z., Ölmez, H., 1996. The influence of ethanolamines on the hydration and mechanical properties of Portland cement. Cement Concr. Res. 26, 701–705. https://doi.org/10.1016/S0008-8846(96)85007-1.

Huang, H., Li, X.R., Avet, F., Hanpongpun, W., Scrivener, K., 2021. Strength-promoting mechanism of alkanolamines on limestone-calcined clay cement and the role of sulfate. Cement Concr. Res. 147, 106527. https://doi.org/10.1016/j.cemconres.2021.106527.

Ji, L., Yu, H., Li, K.K., Yu, B., Grigore, M., Yang, Q., Wang, X.L., Chen, Z.L., Zeng, M., Zhao, S.F., 2018. Integrated absorption-mineralisation for low-energy CO_2 capture and sequestration. Appl. Energy 225, 356–366. https://doi.org/10.1016/j.apenergy.2018.04.108.

Jiang, J., Ye, Z.M., Wu, J.M., Yang, Q.C., Li, Q.L., Kong, X.M., 2024. Impact of triethanolamine on the hydration of Portland cement in the presence of high pozzolanic activity supplementary cementitious materials. Cem. Concr. Compos. 147, 105435. https://doi.org/10.1016/j.cemconcomp.2024.105435.

Lang, L., Zhu, M., Pu, S., 2025. Recycling engineering sediment waste as sustainable subgrade material using ground granulated blast-furnace slag, electrolytic manganese residue and cement. Environ. Technol. Innov. 37, 103969. https://doi.org/10.1016/j.eti.2024.103969.

Li, W., Hua, L.M., Shi, Y.L., Wang, P.G., Liu, Z.C., Cui, D.B., Sun, X.G., 2022. Influence of metakaolin on the hydration and microstructure evolution of cement paste during the early stage. Appl. Clay Sci. 229, 106674. https://doi.org/10.1016/j.clay.2022.106674.

Li, S.C., Wang, D.X., Tang, C.Y., Chen, Y.R., 2023a. Optimization of synergy between cement, slag, and phosphogypsum for marine soft clay solidification. Constr. Build. Mater. 374, 130902. https://doi.org/10.1016/j.conbuildmat.2023.130902.

Li, W.T., Chen, Y., Li, R.X., Xiao, H.L., Li, L.H., Yang, J.T., 2023b. A new method for carbonating magnesia and its possible application to soil stabilization and CO_2 capture. Constr. Build. Mater. 383, 131263. https://doi.org/10.1016/j.conbuildmat.2023.131263.

Li, M., Cai, G.J., Wang, Q., Liu, S.Y., He, H., Liu, X.W.Y., Shi, W., 2023c. The state of the art of carbonation technology in geotechnical engineering: a comprehensive review. Renew. Sustain. Energy Rev. 171, 112986. https://doi.org/10.1016/j.rser.2022.112986.

Liu, J., Hu, L., Tang, L.P., Ren, J., 2021a. Utilisation of municipal solid waste incinerator (MSWI) fly ash with metakaolin for preparation of alkali-activated cementitious material. J. Hazard. Mater. 402, 123451. https://doi.org/10.1016/j.jhazmat.2020.123451.

Liu, S.Y., Cai, G.H., Du, G.Y., Wang, L., Li, J.S., Qian, X.C., 2021b. Field investigation of shallow soft-soil highway subgrade treated by mass carbonation technology. Can. Geotech. J. 58, 97–113. https://doi.org/10.1139/cgj-2020-0008.

Liu, J., Xie, G.M., Wang, Z.D., Li, Z.L., Fan, X., Jin, H.S., Zhang, W.Z., Xing, F., Tang, L.P., 2023. Synthesis of geopolymer using municipal solid waste incineration fly ash and steel slag: hydration properties and immobilization of heavy metals. J. Environ. Manag. 341, 118053. https://doi.org/10.1016/j.jenvman.2023.118053.

Lu, Z.C., Kong, X.M., Jansen, D., Zhang, C.Y., Wang, J., Pang, X.F., Yin, J.H., 2020. Towards a further understanding of cement hydration in the presence of triethanolamine. Cement Concr. Res. 132, 106041. https://doi.org/10.1016/j.cemconres.2020.106041.

Ma, Z.H., Liao, H.Q., Cheng, F.Q., 2021. Synergistic mechanisms of steelmaking slag coupled with carbide slag for CO_2 mineralization. Int. J. Greenh. Gas Control

105, 103229. https://doi.org/10.1016/j.ijggc.2020.103229.
Meng, F.Z., Meng, Y., Ju, T.Y., Han, S.Y., Lin, L., Jiang, J.G., 2022. Research progress of aqueous amine solution for CO_2 capture: a review. Renew. Sustain. Energy Rev. 168, 112902. https://doi.org/10.1016/j.rser.2022.112902.
Ministry of Water Resource, 2008. GB/T 4935.1 Instrument for Soil test-oedometer-part 1: Single Level Arm Oedometer.
Phan, H.Q.H., Hwang, K.Y., Ahn, J.Y., Kim, T.Y., Kim, C., Hwang, I., 2017. Investigation of the accelerated carbonation of a MgO-based binder used to treat contaminated sediment. Environ. Earth Sci. 76, 771. https://doi.org/10.1007/s12665-017-7115-6.
Phetchuay, C., Horpibulsuk, S., Arulrajah, A., Suksiripattanapong, C., Udomchai, A., 2016. Strength development in soft marine clay stabilized by fly ash and calcium carbide residue based geopolymer. Appl. Clay Sci. 127, 134–142. https://doi.org/10.1016/j.clay.2016.04.005.
Provis, J.L., Bernal, S.A., 2014. Geopolymers and related alkali-activated materials. Annu. Rev. Mater. Res. 44, 299–327. https://doi.org/10.1146/annurev-matsci-070813-113515.
Qiu, Y., Yang, C., Wu, M., Li, J., He, R., Hao, C., Fan, X., 2024. Analysis of emulsion compositionand the migration and transformationin mine water. Pol. J. Environ. Stud. 33, 4297–4309. https://doi.org/10.15244/pjoes/177151.
Ruan, S., Unluer, C., 2016. Comparative life cycle assessment of reactive MgO and Portland cement production. J. Clean. Prod. 137, 258–273. https://doi.org/10.1016/j.jclepro.2016.07.071.
Shen, W.G., Cao, L., Li, Q., Zhang, W.S., Wang, G.M., Li, C.C., 2015. Quantifying CO_2 emissions from China's cement industry. Renew. Sustain. Energy Rev. 50, 1004–1012. https://doi.org/10.1016/j.rser.2015.05.031.
Shin, S., Kim, M.J., 2022. Utilization of residual by-products remaining after indirect carbonation: zeolite synthesis and conversion mechanism. J. Environ. Chem. Eng. 10, 108599. https://doi.org/10.1016/j.jece.2022.108599.
Teune, I.E., Schollbach, K., 2024. Triethanolamine-promoted separation of calcium from recycled concrete fines during aqueous carbonation. Resour. Conserv. Recycl. 206, 107604. https://doi.org/10.1016/j.resconrec.2024.107604.
Van Roijen, E., Sethares, K., Kendall, A., Miller, S.A., 2024. The climate benefits from cement carbonation are being overestimated. Nat. Commun. 15, 4848. https://doi.org/10.1038/s41467-024-48965-z.
Wang, D.X., Xiao, J., Gao, X.Y., 2019a. Strength gain and microstructure of carbonated reactive MgO-fly ash solidified sludge from east Lake, China. Eng. Geol. 251, 37–47. https://doi.org/10.1016/j.enggeo.2019.02.012.
Wang, D.X., Xiao, J., He, F.J., Zhou, Y.D., 2019b. Durability evolution and associated micro-mechanisms of carbonated reactive MgO-fly ash solidified sludge from East Lake, China. Constr. Build. Mater. 208, 1–12. https://doi.org/10.1016/j.conbuildmat.2019.02.173.
Wang, D.X., Zhu, J.Y., He, F.J., 2019c. Quantification and micro-mechanisms of CO_2 sequestration in magnesia-lime-fly ash/slag solidified soils. Int. J. Greenh. Gas Control 91, 102827. https://doi.org/10.1016/j.ijggc.2019.102827.
Wang, Z.S., Wang, D.X., 2023. Durability of industrial by-products combined with cement-solidified sludge subjected to immersion and cyclic wetting-drying in various fluids. ACTA Geotech. 18, 6849–6874. https://doi.org/10.1007/s11440-023-01949-7.
Wang, Y.T., Zhao, X., Cao, P.Y., Zhang, Z.Y., Liu, J.X., 2023. Effect of triethanolamine on the initial setting time and hydration behavior of BOFS - cement materials. J. Build. Eng. 78, 107751. https://doi.org/10.1016/j.jobe.2023.107751.
Wang, Q., Cheng, Y.J., Cai, G.J., Guo, J.W., Li, Y.F., 2024. Experimental analysis of mechanical properties of dredged sludge solidified by carbonized under the synergistic action of magnesium oxychloride cement and lime. Constr. Build. Mater. 447, 138095. https://doi.org/10.1016/j.conbuildmat.2024.138095.
Wang, D.X., Duan, Z.Y., Xiao, J., Zhang, D., Deng, B.W., 2025. Strength and microstructural development of reactive MgO–blast furnace slag solidified sludge subjected to CO_2 carbonation. J. Mater. Civ. Eng. 37 (6), 04025140. https://doi.org/10.1061/JMCEE7/MTENG-19144.
West, R.J., Gonsior, S.J., 1996. Biodegradation of triethanolamine. Environ. Toxicol. Chem. 15, 472–480. https://doi.org/10.1002/etc.5620150410.
Xi, F.M., Davis, S.J., Ciais, P., Crawford-Brown, D., Guan, D.B., Pade, C., Shi, T.M., Syddall, M., Lv, J., Ji, L.Z., Bing, L.F., Wang, J.Y., Wei, W., Yang, K.H., Lagerblad, B., Galan, I., Andrade, C., Zhang, Y., Liu, Z., 2016. Substantial global carbon uptake by cement carbonation. Nat. Geosci. 9, 880–883. https://doi.org/10.1038/ngeo2840.
Xin, P.H., Liu, H., Wang, J.F., Wang, Y.L., Wang, H., Cui, S.P., 2024. Effects of CO_2-absorbed triethanolamine solutions on strength development of cement mortars and the mechanism: synergism of cement hydration and carbonation. Constr. Build. Mater. 413, 134708. https://doi.org/10.1016/j.conbuildmat.2023.134708.
Xu, Z.Q., Li, W.F., Sun, J.F., Hu, Y.Y., Xu, K., Ma, S.H., Shen, X.D., 2017. Research on cement hydration and hardening with different alkanolamines. Constr. Build. Mater. 141, 296–306. https://doi.org/10.1016/j.conbuildmat.2017.03.010.
Yaphary, Y.L., Yu, Z.C., Lam, R.H.W., Lau, D., 2017. Effect of triethanolamine on cement hydration toward initial setting time. Constr. Build. Mater. 141, 94–103. https://doi.org/10.1016/j.conbuildmat.2017.02.072.
Yi, Y.L., Lu, K.W., Liu, S.Y., Al-Tabbaa, A., 2016. Property changes of reactive magnesia-stabilized soil subjected to forced carbonation. Can. Geotech. J. 53, 314–325. https://doi.org/10.1139/cgj-2015-0135.
Yu, C.Y., Cui, C.Y., Wang, Y., Zhao, J.Y., Wu, Y.J., 2021. Strength performance and microstructural evolution of carbonated steel slag stabilized soils in the laboratory scale. Eng. Geol. 295, 106410. https://doi.org/10.1016/j.enggeo.2021.106410.
Yu, C.Y., Cui, C.Y., Zhao, J.Y., Zheng, J.J., 2022. Carbonation properties of dredged slurry pre-dried with steel slag powder: effects of clay minerals and organic acids. Constr. Build. Mater. 353, 129096. https://doi.org/10.1016/j.conbuildmat.2022.129096.
Yu, C., Cui, C., Zhao, J., Liu, F., Fu, S., Li, G., 2024. Enhancing mechanical properties of dredged sludge through carbonation stabilization employing steel slag: an eco-friendly and cost-effective approach. Constr. Build. Mater. 412, 134748. https://doi.org/10.1016/j.conbuildmat.2023.134748.
Zajac, M., Irbe, L., Bullerjahn, F., Hilbig, H., Ben Haha, M., 2022. Mechanisms of carbonation hydration hardening in Portland cements. Cement Concr. Res. 152, 106687. https://doi.org/10.1016/j.cemconres.2021.106687.
Zhang, Y.R., Kong, X.M., Lu, Z.C., Lu, Z.B., Zhang, Q., Dong, B.Q., Xing, F., 2016. Influence of triethanolamine on the hydration product of portlandite in cement paste and the mechanism. Cement Concr. Res. 87, 64–76. https://doi.org/10.1016/j.cemconres.2016.05.009.

Dr. Dongxing Wang is currently full Professor and PhD supervisor of School of Civil Engineering, Wuhan University. He obtained the PhD degree from Lille 1 University of Science and Technology, France. From September 2018 to December 2019, he was a visiting scholar at Royal Institute of Technology, Sweden. He is an editorial board member and a guest editor of *Marine Georesources and Geotechnology*. Especially, he is Distinguished Young Scholar granted by Natural Science Foundation of both Hubei Province and Hunan Province, China. His research interests include solidification/stabilization of problematic soils, ground improvement, tunnel construction, and urban underground space development.